constitutional isomeric libraries of AB_2-based monodendrons and supramolecular dendrimers. *J. Am. Chem. Soc.* **123,** 1302–1315 (2001).
16. Percec, V., Holerca, M. N., Uchida, S., Yeardley, D. J. P. & Ungar, G. Poly(oxazoline)s with tapered minidendritic side groups as models for the design of synthetic macromolecules with tertiary structure. *Biomacromolecules* **2,** 729–740 (2001).
17. Percec, V. *et al.* Exploring and expanding the three-dimensional structural diversity of supramolecular dendrimers with the aid of libraries of alkali metals of their AB_3 minidendritic carboxylates. *Chem. Eur. J.* **8,** 1106–1117 (2002).
18. Gähler, F. in *Quasicrystalline Materials* (eds Janot, C. & Dubois, J. M.) 272–284 (World Scientific, Singapore, 1988).
19. Frank, F. C. & Kasper, J. S. Complex alloy structures regarded as sphere packing. I. Definitions and basic principles. *Acta Crystallogr.* **11,** 184–190 (1958).
20. Ishimasa, T., Nissen, H.-U. & Fukano, Y. New ordered state between crystalline and amorphous in Ni-Cr particles. *Phys. Rev. Lett.* **55,** 511–513 (1985).
21. Chen, H., Li, D. X. & Kuo, K. H. New type of two-dimensional quasicrystal with twelvefold rotational symmetry. *Phys. Rev. Lett.* **60,** 1645–1648 (1988).
22. Yoshida, K., Yamada, T. & Taniguchi, Y. Long-period tetragonal lattice formation by solid-state alloying at the interfaces of Bi-Mn double-layer thin-films. *Acta Crystallogr. B* **45,** 40–45 (1989).
23. Conrad, M., Krumeich, F. & Harbrecht, B. A dodecagonal quasicrystalline chalcogenide. *Angew. Chem. Int. Edn Engl.* **37,** 1383–1386 (1998).
24. Stampfli, P. A dodecagonal quasiperiodic lattice in two dimensions. *Helv. Phys. Acta* **59,** 1260–1263 (1986).
25. Baake, M., Klitzing, R. & Schlottmann, M. Fractally shaped acceptance domains of quasiperiodic square-triangle tilings with dodecagonal symmetry. *Physica A* **191,** 554–558 (1992).
26. Ziherl, P. & Kamien, R. D. Maximizing entropy by minimizing area: Towards a new principle of self-organization. *J. Phys. Chem. B* **105,** 10147–10158 (2001).
27. Thomson, W. On the division of space with minimum partitional area. *Phil. Mag.* **24,** 503–514 (1887).
28. Weaire, D. (ed.) *The Kelvin Problem: Foam Structures of Minimal Surface Area* (Taylor & Francis, London, 1997).
29. Navailles, L., Barois, P. & Nguyen, H. T. X-ray measurement of the twisted grain boundary angle in the liquid crystal analog of the Abrikosov phase. *Phys. Rev. Lett.* **71,** 545–548 (1993).
30. Navailles, L., Pindak, R., Barois, P. & Nguyen, H. T. Structural study of the smectic-C twisted grain boundary phase. *Phys. Rev. Lett.* **74,** 5224–5227 (1995).
31. Bruinsma, R. F., Gelbart, W. M., Reguera, D., Rudnick, J. & Zandi, R. Viral self-assembly as a thermodynamic process. *Phys. Rev. Lett.* **24,** 248101 (2003).
32. Zoorob, M. E., Charlton, M. D. B., Parker, G. J., Baumberg, J. J. & Netti, M. C. Complete photonic bandgaps in 12-fold symmetric quasicrystals. *Nature* **404,** 740–743 (2000).

Supplementary Information accompanies the paper on **www.nature.com/nature**.

Acknowledgements We thank A. Gleeson and P. Baker for assistance with X-ray diffraction experiments. We are grateful to P. A. Heiney, T. C. Lubensky and R. D. Kamien for reading the draft manuscript and for their suggestions. We acknowledge CCLRC for providing synchrotron beamtime. The synthesis part of the work was supported by the NSF.

Competing interests statement The authors declare that they have no competing financial interests.

Correspondence and requests for materials should be addressed to G.U. (g.ungar@sheffield.ac.uk).

Links between salinity variation in the Caribbean and North Atlantic thermohaline circulation

Matthew W. Schmidt[1], Howard J. Spero[1] & David W. Lea[2]

[1]*Department of Geology, University of California, Davis, California 95616, USA*
[2]*Department of Geological Sciences and Marine Science Institute, University of California, Santa Barbara, California 93106, USA*

Variations in the strength of the North Atlantic Ocean thermohaline circulation have been linked to rapid climate changes[1] during the last glacial cycle through oscillations in North Atlantic Deep Water formation and northward oceanic heat flux[2–4]. The strength of the thermohaline circulation depends on the supply of warm, salty water to the North Atlantic, which, after losing heat to the atmosphere, produces the dense water masses that sink to great depths and circulate back south[2]. Here we analyse two Caribbean Sea sediment cores, combining Mg/Ca palaeothermometry with measurements of oxygen isotopes in foraminiferal calcite in order to reconstruct tropical Atlantic surface salinity[5,6] during the last glacial cycle. We find that Caribbean salinity oscillated between saltier conditions during the cold oxygen isotope stages 2, 4 and 6, and lower salinities during the warm stages 3 and 5, covarying with the strength of North Atlantic Deep Water formation[7]. At the initiation of the Bølling/Allerød warm interval, Caribbean surface salinity decreased abruptly, suggesting that the advection of salty tropical waters into the North Atlantic amplified thermohaline circulation and contributed to high-latitude warming.

Today, most of the North Atlantic's subtropical gyre water circulates through the Caribbean Sea before it is transported to the subpolar regions of the North Atlantic via the Gulf Stream[8]. Net evaporation exceeds precipitation in the Atlantic, resulting in freshwater removal of $\sim 0.35 \times 10^6\ m^3\ s^{-1}$ from the Atlantic basin[9]. Because of their influence on North Atlantic surface salinity, the tropical and subtropical Atlantic play an important part in regulating North Atlantic Deep Water (NADW) formation. However, unlike the Gulf of Mexico and North Atlantic, Caribbean salinity is not significantly affected by freshwater runoff and therefore surface salinity primarily reflects the evaporation/precipitation ratio over the western tropical Atlantic. Hence, changes in tropical

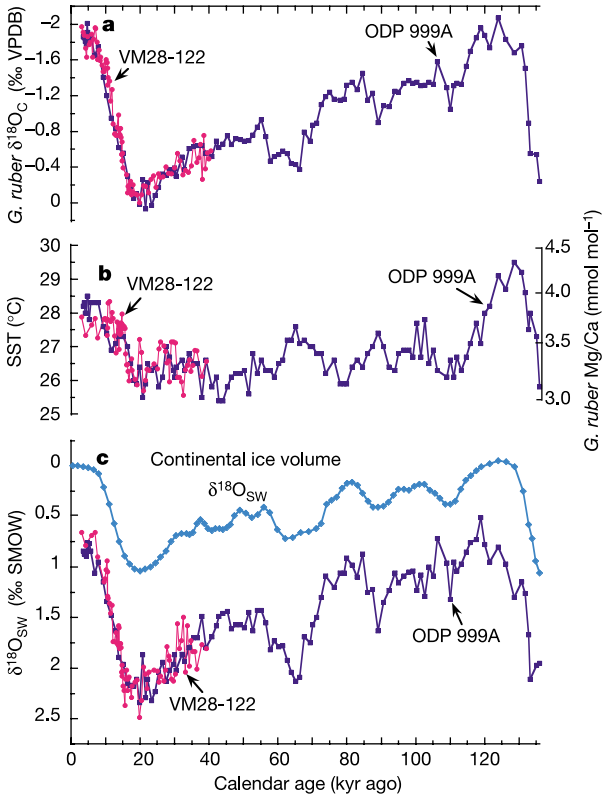

Figure 1 Temperature and $\delta^{18}O_{SW}$ variation in the western Caribbean Sea during the past 136 kyr. **a**, Colombian basin $\delta^{18}O_C$ and **b**, Mg/Ca–SST records from ODP 999A (12° 45′ N, 78° 44′ W; 2,827 m; 4 cm kyr^{-1} sedimentation rate) and VM28-122 (11° 34′ N, 78° 25′ W; 3,623 m; 4 cm kyr^{-1} sedimentation rate during the Holocene and LGM, 10–15 cm kyr^{-1} sedimentation rate during the deglaciation), based on the planktic foraminifer *G. ruber* (white). Mg/Ca was converted to SST[13] using Mg/Ca = 0.38exp0.09[SST–0.61(core depth, in km)]. **c**, Computed $\delta^{18}O_{SW}$ calculated from the Mg/Ca-derived SST and $\delta^{18}O_C$ using T (in °C) = 16.5 − 4.80 (δ_C − (δ_W − 0.27)) (ref. 14). The continental ice-volume $\delta^{18}O_{SW}$ reconstruction[15] is shown for comparison. Note that the amplitude of the calculated $\delta^{18}O_{SW}$ change in the Colombian basin is considerably greater than the global $\delta^{18}O_{SW}$ change due to ice volume alone.

atmospheric circulation have a profound effect on Caribbean surface salinity, which could in turn affect the salinity and density structure of the entire North Atlantic.

The $^{18}O/^{16}O$ ratio of sea water covaries linearly with surface salinity, making it one of the most direct proxies for estimating salinity in the modern ocean[10]. On glacial timescales, the $\delta^{18}O$ value for sea water ($\delta^{18}O_{SW}$) is also affected by variations in continental ice volume because the formation of glacial ice preferentially removes $H_2^{16}O$ from the ocean. The $\delta^{18}O$ of foraminiferal calcite ($\delta^{18}O_C$) is controlled by temperature and $\delta^{18}O_{SW}$, so $\delta^{18}O_{SW}$ can be computed if temperature is determined independently. Initial attempts to compute North Atlantic $\delta^{18}O_{SW}$ used indirect sea surface temperature (SST) estimates based on faunal transfer functions[4]. Given the uncertainties in determining the precise magnitude and timing of SST change from transfer functions and the fact that the computed temperature did not necessarily reflect conditions at the time the foraminiferal shell locked in its $\delta^{18}O_C$ value, the resulting surface salinity reconstructions are only qualitative. Here we combine Mg/Ca measurements (a proxy for the temperature of calcification) and $\delta^{18}O$ analyses of shells from the surface-dwelling foraminifera *Globigerinoides ruber* (white) from the western Caribbean Colombian basin at ODP Site 999A and VM28-122 (see Supplementary Information for core location map) to produce the first continuous record of Caribbean $\delta^{18}O_{SW}$ during the last 136 kyr (Fig. 1). The most significant advantage of Mg palaeothermometry over other temperature determinations is that Mg/Ca is measured on the same organism and mineral phase that carries the $\delta^{18}O$ information. Hence, there is no spatial or temporal ambiguity in the incorporation of the two controlling parameters[5,6] and ambient $\delta^{18}O_{SW}$ can be computed directly.

Age models for ODP 999A and VM28-122 were developed using eight new and six previously published accelerator mass spectroscopy (AMS) ^{14}C dates from *G. ruber* and correlation of the *G. ruber* $\delta^{18}O_C$ records to SPECMAP[11] and to estimates of sea level change from coral U–Th dates[12] (see Supplementary Information).

We convert measured Mg/Ca ratios to SST using a depth-corrected *G. ruber* Mg/Ca–SST calibration for the tropical Atlantic[13] (Fig. 1b). To compute $\delta^{18}O_{SW}$, temperature is then removed from the $\delta^{18}O_C$ record using a temperature–$\delta^{18}O$ relationship that has been field-calibrated for use with *G. ruber* (white)[14] (Fig. 1c). The component of $\delta^{18}O_{SW}$ that is due to changes in regional hydrology during the last glacial cycle was then calculated by subtracting the influence of continental ice volume[15] and subtracting the modern Caribbean surface $\delta^{18}O_{SW}$ value, producing the ice-volume-free residual, $\Delta\delta^{18}O_{IVF\text{-}SW}$, presented as the deviation from modern conditions (Fig. 2a).

The *G. ruber* $\delta^{18}O_C$ record from ODP 999A displays a glacial–interglacial amplitude of 2‰ (Fig. 1a). The Holocene and the interglacial Oxygen Isotope Stage (OIS) 5e attain a minimum value of −2.0‰ and the Last Glacial Maximum (LGM) peaks at 0‰. The $\delta^{18}O_C$ record in VM28-122 is nearly identical to ODP 999A through the past 40 kyr. VM28-122 shows virtually all of the detail contained in a 10–20 cm kyr^{-1} *G. ruber* $\delta^{18}O_C$ record from core M35003-4 in the Tobago basin[16], just east of the Caribbean Sea (Fig. 3a).

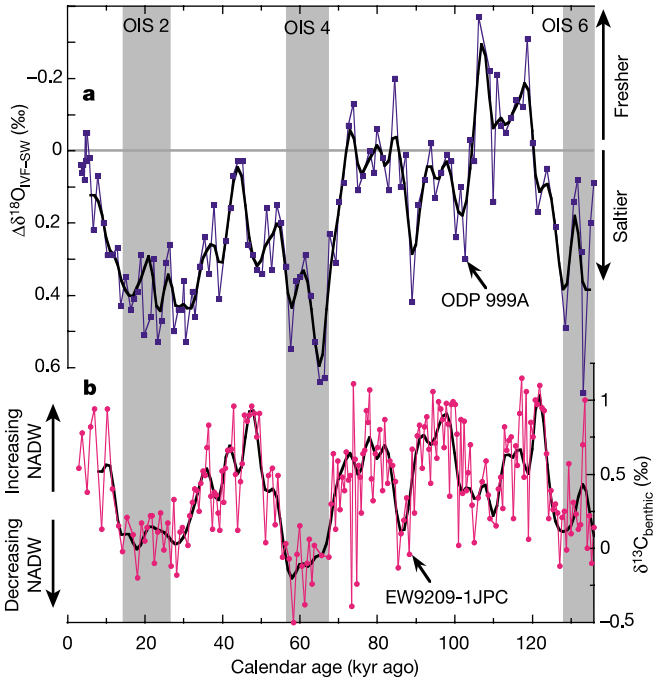

Figure 2 A comparison of local $\delta^{18}O_{SW}$ change in Colombian basin surface water and estimated variation in NADW formation over the past 136 kyr. **a**, $\Delta\delta^{18}O_{IVF\text{-}SW}$ (salinity excess) for ODP 999A represents regional hydrologic changes in the Caribbean through the last glacial cycle. The bold line is a low-pass (5 kyr) filter with a 5-point filter weight running through the raw data (fine line). **b**, Benthic $\delta^{13}C$ record (filtered with a low-pass (5 kyr) filter with a 10-point filter weight) from Ceara Rise core EW9209-1JPC (5° N, 43° W; 4,056 m) indicates times of reduced NADW formation (lower $\delta^{13}C$)[7].

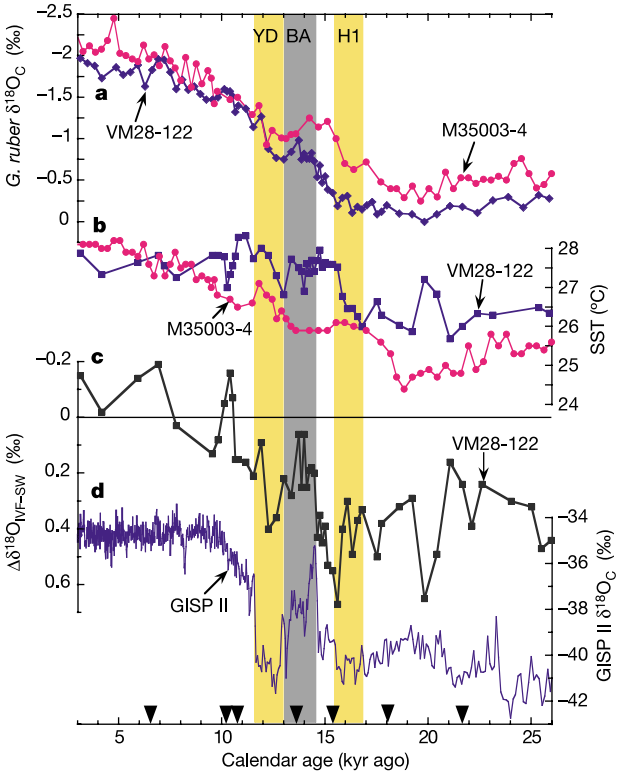

Figure 3 Temperature and salinity variation in the Colombian Basin and in the western tropical Atlantic over the last deglacial. Records of **a**, $\delta^{18}O_C$ and **b**, SST from VM28-122 and from Tobago basin core M35003-4 (12° N, 61° W; 1,299 m) (ref. 16) are compared. $\delta^{18}O_C$ is from *G. ruber* (white) in VM28-122 and from *G. ruber* (pink) in M35003-4. The SST record for VM28-122 is derived from Mg/Ca, whereas the M35003-4 SST record is alkenone-based. The differences in the $\delta^{18}O_C$ and SST records from VM28-122 and M35003-4 may be due to the influence of the low-salinity pool associated with the Amazon and Orinoco river outflow on the Tobago basin or to a southward shift in the glacial NEC. **c**, The computed $\Delta\delta^{18}O_{IVF\text{-}SW}$ record from VM28-122 represents regional surface salinity change in the Caribbean. Note that the rapid salinity decrease in the Caribbean (14.6 kyr ago) corresponds to an increase in the GISP II $\delta^{18}O$ record (**d**)[19] at the beginning of the Bølling/Allerød warm interval. Arrows on the bottom axis indicate VM28-122 intervals with AMS ^{14}C dates. Heinrich Event 1 (H1), the Bølling/Allerød (BA) and the Younger Dryas (YD) are indicated.

The Mg/Ca records from ODP 999A and VM28-122 yield a late Holocene SST of ~28.0 °C and show that the western Caribbean was ~2.5 °C cooler during the LGM (Fig. 1b). These late Holocene SST values agree with the average modern SST for the Colombian basin[17] and the glacial–interglacial temperature difference is consistent with previous estimates for the Caribbean[18]. The SST record from ODP 999A also shows that OIS 4 was ~1.2 °C warmer than OIS 2 and 3. The VM28-122 Mg/Ca record, which has a sedimentation rate of over 15 cm kyr^{-1} during the mid-deglaciation, shows a pause in SST rise associated with the Bølling/Allerød interval[19] (Fig. 3b). This pattern of SST change is similar to that observed from alkenone data in core M35003-4 (ref. 16 and Fig. 3b), but differs from a coastal Cariaco basin SST reconstruction based on Mg/Ca palaeothermometry that indicates significant cooling during the Younger Dryas[20]. Both the Tobago and Cariaco basins yield lower LGM SSTs than the western Caribbean. Because the LGM was a period of enhanced carbonate preservation in the Caribbean, it is unlikely that these LGM temperature differences are due to the influence of dissolution on Mg/Ca in our data. Furthermore, our reported Mg/Ca ratios show a statistically significant negative correlation with average shell weight, suggesting that partial dissolution has not affected our Mg/Ca–SST reconstruction. Rather, the SST difference between the western Caribbean and the eastern sites may be due to a southward shift in the glacial North Equatorial Current (NEC)[21].

Subtracting the influence of SST on *G. ruber* $\delta^{18}O_C$ in ODP 999A and VM28-122, we obtain the salinity proxy, $\delta^{18}O_{SW}$ (Fig. 1c). The late Holocene yields an average $\delta^{18}O_{SW}$ of 0.8‰, in close agreement with modern annual $\delta^{18}O_{SW}$ values for the western Caribbean[22]. The $\delta^{18}O_{SW}$ record for the past 136 kyr has a glacial–interglacial amplitude of ~1.5‰, exceeding estimates of $\delta^{18}O_{SW}$ change due to ice volume by 0.5‰ (ref. 15). Removing the influence of ice volume[15] and subtracting the modern Caribbean surface $\delta^{18}O_{SW}$ value of 0.8‰ yields $\Delta\delta^{18}O_{IVF\text{-}SW}$ (Fig. 2a). Positive values indicate increased surface salinity due to the excess removal of $H_2^{16}O$ during evaporation. In ODP 999A, $\Delta\delta^{18}O_{IVF\text{-}SW}$ was more positive than modern seawater by ~0.5 to 0.6‰ during cold glacial intervals OIS 2, 4 and 6. In contrast, warm OIS 3 and 5 values of $\delta^{18}O_{SW}$ are indistinguishable from the average modern $\delta^{18}O_{SW}$ value in this region (for example, $\Delta\delta^{18}O_{IVF\text{-}SW} \approx 0$). If we assume the freshwater $\delta^{18}O$ value in the tropical Atlantic did not change significantly during the LGM[23], then the modern western Caribbean $\delta^{18}O_{SW}$ to surface salinity relationship, $\delta^{18}O_{SW} = 0.22 \times (\text{surface salinity}) - 6.95$ (ref. 22), is valid for the last glacial cycle. Our glacial $\delta^{18}O_{SW}$ values therefore indicate that Caribbean salinities were 2.3 to 2.7 p.s.u. higher than modern salinities, after the influence of ice volume on oceanic salinity has been subtracted. Previous research also indicates increased western tropical Atlantic surface salinity during glacial periods[24], suggesting a regional increase in glacial surface salinity that extended beyond the Caribbean.

Climate in the modern Colombian basin is characterized by two distinct seasons: a warm, wet season in late summer when the Intertropical Convergence Zone (ITCZ) is located farthest to the north, and a cool, dry season during boreal winter when the ITCZ migrates south[25]. As a result, surface salinity varies seasonally by ~0.7 p.s.u. (ref. 17). The increased glacial salinities calculated in ODP 999A (Fig. 2a) are therefore consistent with modelling[26] and sedimentological data[27] suggesting a southward shift in the ITCZ during periods of reduced NADW formation.

It is generally accepted that cold periods in the North Atlantic are associated with reduced NADW formation[3]. On orbital timescales, benthic foraminiferal $\delta^{13}C$ oscillations from the western tropical Atlantic reflect the relative strength of NADW (high $\delta^{13}C$) and Antarctic Bottom Water (low $\delta^{13}C$) production. Compared with the $\delta^{13}C$ record from western tropical Atlantic Ocean core EW9209-1 JPC[7] over the last glacial cycle (Fig. 2b), reconstructed $\Delta\delta^{18}O_{IVF\text{-}SW}$ from ODP 999A demonstrates that elevated Caribbean salinities occurred when NADW production was reduced. The combined evidence of arid atmospheric conditions[27] and covariation between benthic $\delta^{13}C$ and $\Delta\delta^{18}O_{IVF\text{-}SW}$ during the last glacial cycle suggests that increased glacial Caribbean salinities were a function of both tropical Atlantic hydrological changes and a general decrease in flow rate through the Caribbean that resulted in a weaker Gulf Stream[28].

Comparison of the VM28-122 $\Delta\delta^{18}O_{IVF\text{-}SW}$ record with the GISP II $\delta^{18}O$ record[19] (Fig. 3c, d) reveals that Caribbean surface salinity decreased rapidly at the onset of the Bølling/Allerød interval. The $\delta^{18}O_{SW}$ transition from glacial to modern salinity (as determined by the midpoint of the VM28-122 $\Delta\delta^{18}O_{IVF\text{-}SW}$ transition) occurs during a period of increased sedimentation rate and is coincident with the onset of the Bølling/Allerød at 14.6 kyr ago. During the brief period of Bølling/Allerød warmth in the North Atlantic, Colombian basin salinity reduced significantly, reaching a minimum between 14.5 and 13.7 kyr ago. Both the initiation and termination of this surface-salinity minimum are bracketed by AMS dates. Sedimentological evidence from the Cariaco basin also suggests a rapid northward migration of the ITCZ during the Bølling/Allerød, resulting in enhanced rainfall in the Caribbean region[27]. This salinity decrease was preceded by a brief period of very salty conditions in the Caribbean that could be related to the collapse of thermohaline circulation during Heinrich Event 1 (Fig. 3c). The observed pattern of millennial-scale surface salinity change suggests that cold stadial events are characterized by a drier western tropical Atlantic combined with reduced surface flow through the Caribbean. These surface-salinity reconstructions agree with Cariaco basin sedimentological data but contradict an earlier interpretation that interstadials are periods of increased salinity in the western tropical Atlantic[27].

Recent modelling studies suggest the initiation of the Bølling/Allerød warming and concurrent strengthening of North Atlantic thermohaline circulation was triggered by either a reduction in Southern Ocean salinity due to meltwater pulse 1A[29] or warming and sea-ice retreat[30]. It has been difficult to explain how the warm Bølling/Allerød interval could result from a reinvigoration of thermohaline circulation when North Atlantic surface warming, sea-ice retreat and continental deglaciation should have produced a negative density anomaly that would have reduced deep convection. We hypothesize that excess salt advected from the Caribbean at ~14.6 kyr ago (Fig. 3c) may have helped to offset the low-salinity conditions in the North Atlantic. Model results suggest that the Indian Ocean was an additional source of salt to the North Atlantic at the start of the deglaciation[30]. When combined, these two sources of salt would serve as a density amplifier for deep thermohaline circulation, thereby offsetting the effect of rising temperature and melting ice.

It is clear that the tropical oceans play a key role in glacial–interglacial climate transitions. Because the accumulation of excess salt in the tropical North Atlantic ultimately impacts the density of high-latitude surface waters, it affects North Atlantic climate through its influence on thermohaline circulation. On the basis of our results, surface waters in the Caribbean became exceptionally salty during glacial intervals over the last 136 kyr. Amplification of North Atlantic thermohaline circulation associated with warm phases during glacial cycles may be critically dependent on the delivery of salty waters that accumulate in the Caribbean during cold periods. These results suggest that the tropical hydrologic cycle has a direct role in regulating rapid climate change. □

Methods

Sediment from each core interval was disaggregated in ultrapure water, sieved and dried at 45 °C. To minimize intraspecific variation in shell geochemistry at each core interval, specimens of *G. ruber* s.s. (white) were only collected from the 250–350 μm size fraction. On the basis of preliminary analyses of the intraspecific oxygen isotope variability among *G. ruber* within core intervals, we used 25 shells per stable isotope analysis for all downcore measurements. Samples were collected at 5 cm resolution (ODP 999A) and 2 cm resolution (VM28-122). Samples for stable isotopes were sonicated in methanol for 5–10 s, roasted under vacuum at 375 °C for 30 min, and analysed on a Fisons Optima IRMS, using

an Isocarb common acid bath autocarbonate system at 90 °C at the University of California Davis.

Mg/Ca ratios were measured on foraminifera collected from the same population and size fraction that was used for the stable isotope analyses. Approximately 600 μg of material per sample (~55 shells) was cleaned for trace and minor element analysis[5]. Briefly, samples underwent a multi-step process consisting of initial rinses in ultrapure water, followed by treatments with hot reducing and oxidizing solutions, transfers into new acid-leached micro-centrifuge vials, and finally leaches with a dilute ultrapure acid solution. All sample cleaning was conducted in laminar flow benches under trace-metal-clean conditions. Samples were then dissolved and analysed on a Finnigan Element-2 ICPMS at the University of California Santa Barbara using established procedures[5]. A full suite of trace- and minor-element measurements were made on each sample including Ca, Mg, Sr, Na, Cd, Ba, La, Ce, Nd, Eu, Lu, U, Al, Mn and Fe.

Elemental ratios of Fe/Ca and Al/Ca were used to monitor cleaning efficacy. Analyses with anomalously high Fe/Ca or Al/Ca ratios and/or with recovery of less than 20% after cleaning were rejected. Although Fe/Ca ratios gradually increased with depth in both cores, Al/Ca ratios remained uniformly low, typically $<7\ \mu mol\ mol^{-1}$ in ODP 999A and $<14\ \mu mol\ mol^{-1}$ in VM28-122, indicating that Mg contamination associated with detrital sediment in cleaned samples was not an issue at either site. Although Fe/Ca and Mn/Ca were higher in VM28-122, Mg/Ca did not correlate with Fe/Ca, Al/Ca or Mn/Ca in either core, indicating that the mineral phases containing these metals in the cleaned samples did not affect Mg/Ca ratios in the foraminiferal calcite.

Error analysis

Analytical precision for the $\delta^{18}O_C$ measurements is better than ±0.06‰. The pooled standard deviation of replicate Mg/Ca analyses from ODP 999A was ±1.7% (1 s.d., d.f. = 110). The pooled standard deviation of replicate Mg/Ca analyses from VM28-122 was ±2.4% (1 s.d., d.f. = 129). The overall precision of replicates in this study is slightly better than other tropical cores (typically ~3%)[5,20], most probably reflecting the stability of the water column in the Colombian basin through the last glacial cycle. Standard deviation for the $\delta^{18}O_{SW}$ residual was calculated to be ± 0.2‰, using Monte Carlo methodology that assumed a 1σ normal distribution in the $\delta^{18}O_C$ and Mg/Ca measurements and in the Mg/Ca–SST and $\delta^{18}O$–SST calibrations.

Received 24 October 2003; accepted 19 January 2004; doi:10.1038/nature02346.

1. Boyle, E. A. Is ocean thermohaline circulation linked to abrupt stadial/interstadial transitions? *Quat. Sci. Rev.* **19,** 255–272 (2000).
2. Broecker, W. S., Bond, G., Klas, M., Bonani, G. & Wolfli, W. A salt oscillator in the glacial Atlantic? The concept. *Paleoceanography* **5,** 469–478 (1990).
3. Keigwin, L. D. & Boyle, E. A. Surface and deep ocean variability in the northern Sargasso Sea during marine isotope stage 3. *Paleoceanography* **14,** 164–170 (1999).
4. Duplessy, J. C. *et al.* Changes in surface salinity of the North Atlantic Ocean during the last deglaciation. *Nature* **358,** 485–488 (1992).
5. Lea, D. W., Pak, D. K. & Spero, H. J. Climate impact of Late Quaternary equatorial Pacific sea surface temperature variations. *Science* **289,** 1719–1724 (2000).
6. Elderfield, H. & Ganssen, G. Past temperature and $\delta^{18}O$ of surface ocean waters inferred from foraminiferal Mg/Ca ratios. *Nature* **405,** 442–445 (2000).
7. Curry, W. B. & Oppo, D. W. Synchronous high-frequency oscillations in tropical sea surface temperatures and North Atlantic deep water production during the last glacial cycle. *Paleoceanography* **12,** 1–14 (1997).
8. Johns, W. E., Townsend, T. L., Fratantoni, D. M. & Wilson, W. D. On the Atlantic inflow to the Caribbean Sea. *Deep-Sea Res. I* **49,** 211–243 (2002).
9. Broecker, W. S., Peng, T. H., Jouzel, J. & Russell, G. The magnitude of global fresh-water transports of importance to ocean circulation. *Clim. Dyn.* **4,** 73–79 (1990).
10. Craig, H. & Gordon, L. I. in *Stable Isotopes in Oceanographic Studies and Paleotemperatures* (ed. Tongiorgi, E.) 9–130 (CNR, Pisa, 1965).
11. Bassinot, F. C. *et al.* The astronomical theory of climate and the age of the Brunhes-Matuyama magnetic reversal. *Earth Planet. Sci. Lett.* **126,** 91–108 (1994).
12. Chappell, J. *et al.* Reconciliation of late Quaternary sea levels derived from coral terraces at Huon Peninsula with deep sea oxygen isotope records. *Earth Planet. Sci. Lett.* **141,** 227–236 (1996).
13. Dekens, P. S., Lea, D. W., Pak, D. K. & Spero, H. J. Core top calibration of Mg/Ca in tropical foraminifera: refining paleotemperature estimation. *Geochem. Geophys. Geosyst.* **3,** no. 1022 (2002).
14. Thunell, R., Tappa, E., Pride, C. & Kincaid, E. Sea-surface temperature anomalies associated with the 1997–1998 El Niño recorded in the oxygen isotope composition of planktonic foraminifera. *Geology* **27,** 843–846 (1999).
15. Waelbroeck, C. *et al.* Sea-level and deep water temperature changes derived from benthic foraminifera isotopic records. *Quat. Sci. Rev.* **21,** 295–305 (2002).
16. Ruhlemann, C., Mulitza, S., Muller, P. J., Wefer, G. & Zahn, R. Warming of the tropical Atlantic ocean and slowdown of thermohaline circulation during the last deglaciation. *Nature* **402,** 511–514 (1999).
17. Conkright, M. *et al. NODC Internal Report* at ⟨http://iridl.ldeo.columbia.edu/SOURCES/.NOAA/.NODC/.WOA98/⟩ (NODC, Silver Springs, Maryland, 1998).
18. Hastings, D. W., Russell, A. D. & Emerson, S. R. Foraminiferal magnesium in *Globigerinoides sacculifer* as a paleotemperature proxy. *Paleoceanography* **13,** 161–169 (1998).
19. Grootes, P. M. & Stuiver, M. Oxygen 18/16 variability in Greenland snow and ice with 10^3 to 10^5-year time resolution. *J. Geophys. Res.* **102,** 26455–26470 (1997).
20. Lea, D. W., Pak, D. K., Peterson, L. C. & Hughen, K. A. Synchroneity of tropical high latitude Atlantic temperatures over the last glacial termination. *Science* **301,** 1361–1364 (2003).
21. Vink, A. *et al.* Shifts in the position of the North Equatorial Current and rapid productivity changes in the western Tropical Atlantic during the last glacial. *Paleoceanography* **16,** 1–12 (2001).
22. Watanabe, T. A., Winter, A. & Oba, T. Seasonal changes in sea surface temperature and salinity during the Little Ice Age in the Caribbean Sea deduced from Mg/Ca and 18O/16O ratios in corals. *Mar. Geol.* **173,** 21–35 (2001).
23. Jouzel, J., Hoffmann, G., Koster, R. D. & Masson, V. Water isotopes in precipitation: data/model comparison for present-day and past climates. *Quat. Sci. Rev.* **19,** 363–379 (2000).
24. Dürkoop, A., Hale, W., Mulitza, S., Patzold, J. & Wefer, G. Late Quaternary variations of sea surface salinity and temperature in the western tropical Atlantic: Evidence from $\delta^{18}O$ of *Globigerinoides sacculifer*. *Paleoceanography* **12,** 764–772 (1997).
25. Stidd, C. K. The use of eigenvectors for climate estimates. *J. Appl. Meteorit.* **6,** 255–264 (1967).
26. Vellinga, M. & Wood, R. A. Global climatic impacts of a collapse of the Atlantic thermohaline circulation. *Clim. Change* **54,** 251–267 (2002).
27. Peterson, L. C., Haug, G. H., Hughen, K. A. & Rohl, U. Rapid changes in the hydrologic cycle of the tropical Atlantic during the last Glacial. *Science* **290,** 1947–1951 (2000).
28. Lynch-Stieglitz, J., Curry, W. B. & Slowey, N. Weaker Gulf stream in the Florida Straits during the Last Glacial Maximum. *Nature* **402,** 644–648 (1999).
29. Weaver, A. J., Saaenko, O. A., Clark, P. U. & Mitrovica, J. X. Meltwater pulse 1A from Antarctica as a trigger of the Bolling/Allerod warm interval. *Science* **299,** 1709–1713 (2003).
30. Knorr, G. & Lohmann, G. Southern Ocean origin for the resumption of Atlantic thermohaline circulation during deglaciation. *Nature* **424,** 532–536 (2003).

Supplementary Information accompanies the paper on **www.nature.com/nature**.

Acknowledgements We thank the Ocean Drilling Program (ODP) and the LDEO Deep-Sea Sample Repository for core samples. Laboratory assistance from D. Pak and mass spectrometer operation by G. Paradis and D. Winter were critical to the success of this study. We also thank A. Droxler for providing a suite of his ODP 999A samples, and J. Kennett and A. Russell for their comments and suggestions. Funding for this research was provided by a USSSP Schlanger Ocean Drilling Fellowship to M.W.S. and the US National Science Foundation (H.J.S. and D.W.L.).

Competing interests statement The authors declare that they have no competing financial interests.

Correspondence and requests for materials should be addressed to M.W.S. (schmidt@geology.ucdavis.edu).

Seismic reflection imaging of two megathrust shear zones in the northern Cascadia subduction zone

Andrew J. Calvert

Department of Earth Sciences, Simon Fraser University, 8888 University Drive, Burnaby, British Columbia, V5A 1S6, Canada

At convergent continental margins, the relative motion between the subducting oceanic plate and the overriding continent is usually accommodated by movement along a single, thin interface known as a megathrust[1]. Great thrust earthquakes occur on the shallow part of this interface where the two plates are locked together[2]. Earthquakes of lower magnitude occur within the underlying oceanic plate, and have been linked to geochemical dehydration reactions caused by the plate's descent[3–7]. Here I present deep seismic reflection data from the northern Cascadia subduction zone that show that the inter-plate boundary is up to 16 km thick and comprises two megathrust shear zones that bound a >5-km-thick, ~110-km-wide region of imbricated crustal rocks. Earthquakes within the subducting plate occur predominantly in two geographic bands where the dip of the plate is inferred to increase as it is forced around the edges of the imbricated inter-plate boundary zone. This implies that seismicity in the subducting slab is controlled primarily by deformation in the upper part of the plate. Slip on the shallower megathrust shear zone, which may occur by aseismic slow slip, will transport crustal rocks into the upper mantle above the subducting oceanic plate and may, in part, provide an explanation for the unusually low seismic wave speeds that are observed there[8,9].

The Cascadia subduction zone, where the oceanic Juan de Fuca plate descends beneath the overlying North American plate, extends 1,100 km from northern California to northern Vancouver Island. Sedimentary rocks originally deposited on the oceanic plate are